0026-895X/95/030568-14$3.00/0

MOLECULAR PHARMACOLOGY, 47:568–581, 1995.

In Vitro Pharmacology of ACEA-1021 and ACEA-1031: Systemically Active Quinoxalinediones with High Affinity and Selectivity for *N*-Methyl-D-aspartate Receptor Glycine Sites

R. M. WOODWARD, J. E. HUETTNER, J. GUASTELLA, J. F. W. KEANA, and E. WEBER

Acea Pharmaceuticals Inc., Irvine, California 92715 (R.M.W., J.G.), Department of Cell Biology and Physiology, Washington University School of Medicine, St. Louis, Missouri 63110 (J.E.H.), Department of Chemistry, University of Oregon, Eugene, Oregon 97403 (J.F.W.K.), and Department of Pharmacology, University of California, Irvine, Irvine, California 92717 (E.W.)

Received August 22, 1994; Accepted December 15, 1994

SUMMARY

N-Methyl-D-aspartate (NMDA) receptor antagonists show therapeutic potential as neuroprotectants, analgesics, and anticonvulsants. In this context, we used electrical recording techniques to study the *in vitro* pharmacology of two novel quinoxalinediones, i.e., ACEA-1021 and ACEA-1031 (5-nitro-6,7-dichloro- and 5-nitro-6,7-dibromo-1,4-dihydro-2,3-quinoxalinedione, respectively). Assays with NMDA receptors expressed by rat brain poly(A)$^+$ RNA in *Xenopus* oocytes and with NMDA receptors in cultured rat cortical neurons indicated that ACEA-1021 and ACEA-1031 are potent competitive antagonists at NMDA receptor glycine sites. Apparent dissociation constants (K_b values) for ACEA-1021 and ACEA-1031 ranged between 6 and 8 nM for oocyte assays and between 5 and 7 nM for neuronal assays. Cloned NMDA receptors expressed in oocytes showed up to 50-fold variation in sensitivity, depending upon subunit composition. For example, using fixed agonist concentrations (10 μM glycine and 100 μM glutamate) IC_{50} values for ACEA-1021 with four binary combinations were as follows: NMDA receptor (NR)1A/2A, 29 nM; NR1A/2B, 300 nM; NR1A/2C, 120 nM; NR1A/2D, 1500 nM. Measurement of EC_{50} for glycine and calculation of K_b for the inhibitors indicated that differences in IC_{50} values are due to subunit-dependent variations in glycine affinity (EC_{50} ranged between ~0.1 and 1 μM) combined with variations in affinity of the antagonists themselves (K_b of ~2–13 nM). In addition to the strong antagonism of NMDA receptors, ACEA-1021 and ACEA-1031 were also moderately potent competitive inhibitors of non-NMDA receptors activated either by α-amino-3-hydroxy-5-methylisoxazole-4-propionic acid or by kainate. Antagonist affinities were similar whether measured with receptors expressed by rat brain poly(A)$^+$ RNA in oocytes (K_b of 1–2 μM) or with cultured neurons (K_b of 1.5–3.3 μM). Our results suggest that the *in vivo* neuroprotective actions of ACEA-1021 and ACEA-1031 are predominantly due to inhibition at NMDA receptor glycine sites, although additional inhibition at non-NMDA receptors may play an ancillary role.

Channel gating at NMDA receptors is effected by two ligands, glutamate and glycine, acting in conjunction at distinct binding sites (1). Experiments in *Xenopus* oocytes and cultured neurons suggest that NMDA by itself causes only low levels of channel activation, indicating that glycine should be considered a "coagonist" at NMDA receptors (2–4). Although details remain uncertain, evidence from electrophysiological and biochemical studies suggests that glycine and glutamate binding sites are allosterically coupled (e.g., Refs. 5 and 6) and that glycine reduces one form of receptor desensitization by increasing the rate of recovery from desensitized states (4, 7).

Studies at the molecular level have revealed a diversity of NMDA receptor subunits, implying that a number of different receptor subtypes are present in mammalian nervous systems (8). This is supported by binding studies and physiological evidence indicating that, depending on brain region and stage of development, NMDA receptors can show different pharmacologies or electrical properties (e.g., Refs. 5 and 9). At present, two classes of subunit have been identified, (i) NR1 subunits, which are found in eight different isoforms generated by alternative RNA splicing (10, 11), and (ii) NR2 subunits, which are found in four distinct subtypes, each encoded by a separate gene (12–14). NR1A (adopting the terminology used in Ref. 11) appears to be the predominant isoform in adult rat brain. Expression studies in oocytes suggest that NR1 subunits are sufficient to produce gluta-

J.E.H. was supported by Grant NS30888 from the National Institutes of Health. J.F.W.K. and E.W. were supported in part by Grant RO1-DA06726 from the National Institute on Drug Abuse.

ABBREVIATIONS: NMDA, *N*-methyl-D-aspartic acid; ACPD, 1-aminocyclopentane-1,3-dicarboxylic acid; AMPA, α-amino-3-hydroxy-5-methylisoxazole-4-propionic acid; BAPTA, 1,2-bis(2-aminophenoxy)ethane-*N*,*N*,*N*′,*N*′-tetraacetic acid; DMSO, dimethylsulfoxide; DNQX, 6,7-dinitroquinoxaline-2,3-dione; 5,7-diClKA, 5,7-dichlorokynurenic acid; EGTA, ethylene glycol bis(β-aminoethyl ether)-*N*,*N*,*N*′,*N*′-tetraacetic acid; HEPES, 4-(2-hydroxyethyl)-1-piperazineethanesulfonic acid; NR1 and NR2, *N*-methyl-D-aspartic acid receptor types 1 and 2.

mate receptors with NMDA-like pharmacology and electrical properties (10, 11). However, levels of functional receptor expression in oocytes are >10-fold higher using combinations of NR1 and NR2 subunits (13), and functional receptor expression in mammalian systems is detectable only with hetero-oligomeric expression (12). This has led to the idea that hetero-oligomeric NMDA receptors more accurately represent the subunit composition of neuronal receptors. For the NR2 subunits, *in situ* hybridization studies indicate strikingly different patterns of localization in adult mammalian brain (12–14). Generally speaking, NR2A and NR2B subunits are strongly expressed in forebrain structures, NR2C in cerebellum, and NR2D in diencephalon and brainstem. Distribution of NR2 subunits also varies during the course of development (14). Taken together, these results raise the possibility that different NMDA receptor subtypes are involved in discrete aspects of brain function and, hence, that subtype-selective drugs should be able to regulate these processes with a degree of specificity.

NMDA receptor antagonists show therapeutic potential as neuroprotectants (15), anticonvulsants (16), and analgesics (17). From a pharmacological perspective the glycine site provides a target for controlling NMDA receptor activity, which, depending on the circumstances, could have advantages over the use of ligands acting via other sites (18, 19). For example, glycine site antagonists do not appear to induce neuronal vacuolation (vacuolization), a phenomenon that has been a cause for concern with other types of antagonists (20), and have relatively encouraging profiles of behavioral side effects (21, 22). Glycine site antagonists can be divided into a variety of classes (see Refs. 18, 19, and 23 for reviews), (i) partial agonists and related compounds, (ii) kynurenic acids, thiokynurenic acids, and the structurally related 2-carboxytetrahydroquinolines, (iii) indole-2-carboxylic acids, (iv) dihydro-2,5-dioxo-3-hydroxy-1*H*-benzazepines (24), (v) quinoxalinediones and related compounds (25–28), and (vi) 3-acyl-4-hydroxy-, 3-nitro-3,4-dihydro-, and 3-phenyl-4-hydroxyquinolin-2(1*H*)-ones (29–31). The different classes of antagonists show a wide range of potencies, selectivities, and *in vivo* bioavailability (19, 29, 31).

Quinoxaline-2,3-diones were initially described as selective ligands for the non-NMDA (AMPA/kainate) family of glutamate receptors (3, 25, 27, 32). Molecules of this class are usually considered to be moderate or low potency ligands at NMDA receptor glycine sites, with modest levels of selectivity between NMDA and non-NMDA receptors and little ability to penetrate the blood/brain barrier (3, 25–28, 32, 33). We report on two quinoxalinediones that contradict many of these conceptions, i.e., ACEA-1021 (5-nitro-6,7-dichloro-1,4-dihydro-2,3- quinoxalinedione) and the structurally related molecule ACEA-1031 (5-nitro-6,7-dibromo-1,4-dihydro-2,3-quinoxalinedione) (Fig. 1). Pharmacological characterization of ACEA-1021 and ACEA-1031 has been prompted by concurrent studies that indicate that both compounds have systemic bioavailability and are efficacious as neuroprotectants in rat focal ischemia models of stroke (34). Furthermore, ACEA-1021 does not appear to substitute for phencyclidine in drug discrimination studies (35).

In the present study two assay systems were used to characterize the basic *in vitro* pharmacology of ACEA-1021 and ACEA-1031 at mammalian glutamate receptors, (i) *Xenopus* oocytes, where drug potencies were assayed against NMDA, non-NMDA, and metabotropic receptors expressed by rat brain poly(A)$^+$ RNA and four putative NMDA receptor subtypes expressed by mixtures of subunit-encoding cRNA, and (ii) cultured rat cortical neurons, where ACEA-1021 was assayed against NMDA and non-NMDA receptors. For purposes of comparison, the oocyte studies included 5,7-diClKA, a selective glycine site antagonist, and DNQX, a quinoxaline-2,3-dione showing selectivity for non-NMDA receptors (Fig. 1).

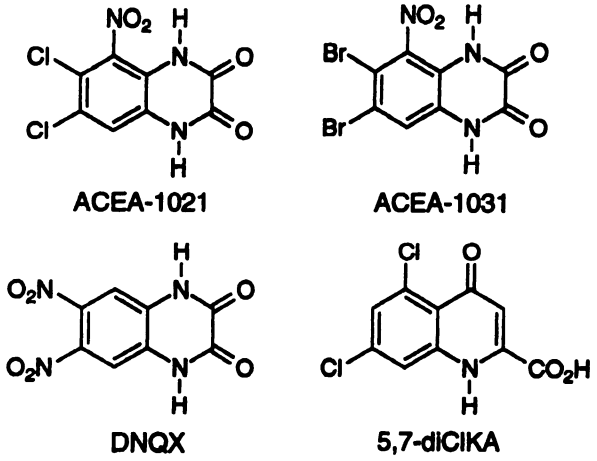

Fig. 1. Structures of ACEA-1021, ACEA-1031, 5,7-diClKA, and DNQX.

Materials and Methods

Preparation of RNA. Total RNA from whole rat brain (including cerebellum and a portion of the brainstem) was prepared using the acid guanidinium/phenol method. Poly(A)$^+$ mRNA was isolated from total cellular RNA by oligo(dT)-cellulose chromatography. All RNA samples were stored in sterile water at −80° until needed.

cDNA clones encoding the NR1A, NR2A, NR2B, NR2C, and NR2D rat NMDA receptor subunits were generously provided by Dr. P. H. Seeburg (Heidelberg University, Heidelberg, Germany). The sequences and some functional properties of these clones, and their mouse homologs, have been reported previously (e.g., Refs. 10, and 12–14). Clones were transformed into appropriate host bacteria and plasmid preparations were made with conventional DNA purification techniques. A sample of each clone was linearized by restriction enzyme digestion and cRNA was synthesized with T3 RNA polymerase. The cRNA was diluted to 400 ng/μl and stored in 1-μl aliquots until injection.

***Xenopus* oocyte expression system.** Following established procedures (36), mature female *Xenopus laevis* were anesthetized (20–40 min) using 0.15% 3-aminobenzoic acid ethyl ester (MS-222), and two to four ovarian lobes were surgically removed. Oocytes at developmental stages V–VI, and still surrounded by enveloping ovarian tissues, were dissected from the ovary. Follicle-enclosed oocytes were microinjected (pipette tip diameter, 20–30 μm) with approximately 50 ng of whole-brain poly(A)$^+$ RNA or with 1:1 mixtures of cRNA (NR1A plus NR2A, -2B, -2C, or -2D; ~2, 5, or 20 ng of RNA encoding each receptor subunit). NR1A-encoding cRNA was injected alone at 20 ng. In general, we aimed to restrict levels of expression such that maximum currents, measured at the second phase, ranged between 100 and 500 nA. Larger responses (e.g., >1 μA) were more susceptible to contamination by secondary Ca^{2+}-gated Cl^- currents. Oocytes were stored in Barth's medium [88 mM NaCl, 1 mM KCl, 0.41 mM $CaCl_2$, 0.33 mM $Ca(NO_3)_2$, 0.82 mM $MgSO_4$, 2.4 mM $NaHCO_3$, 5 mM HEPES, pH 7.4, with 0.1 mg/ml gentamycin sulfate]. While oocytes were still surrounded by enveloping ovarian tissues, the

Barth's medium was supplemented with 0.1% bovine serum. Oocytes were defolliculated 1 day after injection by treatment with collagenase (0.5 mg/ml Sigma type I, for 0.5–1 hr), vortex-mixed to dislodge epithelia, and subsequently stored in serum-free medium.

Electrical recordings were made, using a conventional two-electrode voltage clamp (Dagan TEV-200), over periods ranging between 3 and 14 days after injection. Oocytes were placed in a 0.1-ml recording chamber that was continuously perfused (5–15 ml/min) with frog Ringer solution (115 mM NaCl, 2 mM KCl, 1.8 mM $CaCl_2$, 5 mM HEPES, pH 7.4). Drugs were applied by bath perfusion. The pH of all solutions (particularly AMPA and kainate) was readjusted to 7.4 where necessary. When the more rapid flow rates were used, half-times for mid-chamber solution changes were 2–3 sec. Exchange rates for drug solutions at the oocyte surface (i.e., beneath the vitelline envelope and among the tangles of microvilli) appeared to be considerably longer. Zero-Ca^{2+}/Ba^{2+} Ringer solution was composed of 115 mM NaCl, 2 mM KCl, 1.8 mM $BaCl_2$, 5 mM HEPES, pH 7.4. Intraoocyte injections were made by pneumatic pressure-pulse ejection from micropipettes (37). Injection solutions of EGTA (40–400 mM) and BAPTA (50–500 mM) were made up in H_20, the pH was adjusted to 7.4 with KOH or HCl, and the solutions were filtered to minimize plugging (Acrodisc-13 filters, 0.2-μm pore size). Pressure was set between 200 and 400 kPa. The volume of injections was regulated by adjusting the time of the pulses (0.1–1 sec) and was estimated by measuring the diameters of ejected droplets.

Neuronal recordings. Primary dissociated cultures of cerebral cortical neurons were prepared from newborn rats as described (24). Cultures were used for electrophysiological recordings after 1–3 weeks *in vitro*. The culture dish was perfused at a rate of 1–5 ml/min with Tyrode's solution (150 mM NaCl, 4 mM KCl, 2 mM $CaCl_2$, 2 mM $MgCl_2$, 10 mM glucose, 10 mM HEPES, pH 7.4). Whole-cell pipettes, pulled from Boralex glass capillaries (Rochester Scientific Co.), were filled with an internal solution that contained 5 mM CsCl, 10 mM EGTA, 10 mM HEPES, and either 140 mM $CsCH_3SO_3$ or 140 mM CsF (pH adjusted to 7.4 with CsOH).

Excitatory amino acid agonists and antagonists were applied in an external solution composed of 160 mM NaCl, 2 mM $CaCl_2$, 500 nM tetrodotoxin, and 10 mM HEPES, pH 7.4. The amplitude of agonist-evoked currents were determined relative to the holding current in control external solution, which lacked agonist. For experiments with kainate and AMPA, 1 μM dizocilpine (MK-801) was added to the external solution to ensure blockade of NMDA receptor channels. Drug solutions were applied to the neurons from a linear array of microcapillary tubes (2-μl Drummond Microcaps, 55-mm length). The time constant for external solution exchange ranged from 30 to 100 msec. Whole-cell currents were recorded with an Axopatch 200 amplifier (Axon Instruments). Currents were filtered at 1–5 kHz (−3 dB, four-pole Bessel filter), digitized at 5 kHz, and stored on computer. Steady state currents were measured by averaging 1–5 sec of data during the final third of each agonist application. Membrane potentials have been corrected for a junction potential of −10 mV between the internal solution and the Tyrode's solution used to perfuse the bath.

Data analysis. Agonist concentration-response curves were analyzed as described previously (24). The logistic equation (eq. 1) was fit to the data for individual concentration-response relations by adjusting the slope factor, n, and the parameter pEC_{50} (pEC_{50} = −log EC_{50}, where EC_{50} is the agonist concentration that produces a half-maximal response) (Sigmaplot; Jandel Scientific).

$$\frac{I}{I_{max}} = \frac{1}{1 + (10^{-pEC_{50}}/[\text{agonist}])^n} \quad (1)$$

Apparent dissociation constants for the antagonists (K_b values) were determined from a simultaneous fit of concentration-response data in the presence and absence of inhibitor, using eq. 2.

$$\frac{I}{I_{max}} = \frac{1}{1 + \left(\frac{10^{-pEC_{50}}\left(\frac{1 + [\text{antagonist}]}{10^{-pK_b}}\right)}{[\text{agonist}]}\right)^n} \quad (2)$$

Concentration-inhibition curves were fit with eq. 3,

$$\frac{I}{I_{control}} = \frac{1}{1 + ([\text{antagonist}]/10^{-pIC_{50}})^n} \quad (3)$$

in which $I_{control}$ is the current evoked by the agonist alone, pIC_{50} is −log IC_{50} (IC_{50} is the concentration of antagonist that produces half-maximal inhibition), and n is the slope factor. The K_b values for antagonists were determined from inhibition curves using a Leff-Dougall generalized form of the Cheng-Prusoff equation (38), eq. 4.

$$K_b = \frac{IC_{50}}{\{2 + ([\text{agonist}]_f/EC_{50})^b\}^{1/b} - 1} \quad (4)$$

where $[\text{agonist}]_f$ is the fixed dose of agonist used to construct the inhibition curve, EC_{50} is the half-maximal agonist concentration, and b is the slope factor of the agonist concentration-response relation. In practice, the parameter $10^{-pIC_{50}}$ was replaced in eq. 3 by $(10^{-pK_b})[([2 + ([\text{agonist}]_f/EC_{50})^b]^{1/b}) - 1]$, where n and pK_b (−log K_b) were the two free parameters. The 95% confidence intervals for pEC_{50}, pIC_{50}, and pK_b were obtained as the product of the standard deviation for each parameter times the appropriate value from the t distribution. In text and tables, confidence intervals have been transformed to a linear scale. Unless otherwise stated, all data quoted in the text are given as mean ± standard error.

Inhibition curve experiments were useful for side-by-side assays of the effects of different antagonists on a common response and, in the case of cloned NMDA receptors, for assessing the relative activity (IC_{50} values) of inhibitors at receptor subtypes with different agonist affinities. Concentration-response (Schild-type) experiments were necessary to investigate the mechanism of inhibition. In most cases, K_b values were calculated using both approaches.

Statistical conformity to the simple competitive model was tested by calculating ratios of residual variance according to eq. 5.

$$F_{df_2-df_1,df_1} = \frac{(SS_2 - SS_1)/(df_2 - df_1)}{SS_1/df_1} \quad (5)$$

where SS_1 is the sum of squared deviations for individual fits (eq. 1), SS_2 is the sum of squared deviations for the simultaneous fit (eq. 2), df_1 is the degree of freedom (number of data points minus number of fitted parameters) for individual fits, and df_2 is the degree of freedom for the simultaneous fit.

Drugs. ACEA-1021 (m.p. 342–344°) and ACEA-1031 (m.p. 352–354°) were synthesized by nitration of 6,7-dichloro-1,4-dihydroquinoxaline-2,3-dione and 6,7-dibromo-1,4-dihydroquinoxaline-2,3-dione, respectively, using KNO_3 and H_2SO_4. Details will be provided elsewhere.[1] Both drugs gave satisfactory elemental analyses. 5,7-diClKA, DNQX, and AMPA were obtained from Research Biochemicals (Natick, MA). BAPTA (cell-impermeant tetrapotassium salt) was from Molecular Probes (Eugene, OR). All other drugs were from Sigma Chemical Co.

Quinoxalinediones were initially dissolved at concentrations of 10–30 mM in DMSO. Dilutions were then made to generate a series of DMSO stock solutions over the range of 0.3 μM–30 mM. Working solutions were made by 1000–3000-fold dilution of stock solutions into Ringer solution. At these dilutions DMSO alone had no measurable effects on membrane current responses. As a vehicle control we also assayed ACEA-1021 made up as a stock solution in 0.2 M Tris with 0.5% (by volume) Tween-80 and 10% polyethylene glycol. This

[1] J. F. W. Keana and E. Weber, unpublished observations.

formulation showed no difference in potency compared with the DMSO stock solutions. 5,7-diClKA (10 mM) was made up in 10–20 mM NaOH, serial dilutions of stock solutions were in water, and dilutions into Ringer solution had no measurable effect on pH. DMSO stock solutions of quinoxalinediones were stored for up to 4 weeks in the dark at 4° without apparent reductions in potency. Ringer solutions of drugs were made up fresh each day of use.

Results

Electrical Recordings from *Xenopus* Oocytes

NMDA receptors expressed by rat whole-brain poly(A)$^+$ RNA. As reported previously for oocytes expressing rat brain poly(A)$^+$ RNA (2), NMDA (1–100 μM) or glycine (0.1–10 μM) elicited minimal membrane current responses when applied alone but activated large currents when coapplied. Membrane currents activated by NMDA/glycine were inward at a holding potential of −70 mV and followed a relatively complex time course involving an initial spike of current, which decayed within 5–10 sec, followed by a second, more slowly developing, peak (Fig. 2). Repeated exposures to saturating concentrations of agonists resulted in some degree of "run-down" of the response (10–60%), often followed by a gradual increase (data not shown). The intracellular regulatory mechanisms responsible for these long term changes in current amplitudes were not investigated.

In agreement with previous studies (39, 40), the initial spike of current was abolished by switching to zero-Ca^{2+}/Ba^{2+} Ringer solution or by injecting the oocyte with EGTA or BAPTA (100–500 pmol; intraoocyte concentration, ~0.2–1 mM) (37). This confirmed that the response spike is a secondary current due to Ca^{2+} influx through NMDA receptor channels and concomitant activation of endogenous Ca^{2+}-gated Cl^- channels. Interestingly, the slowly developing current peak was largely unaffected by EGTA or BAPTA injections and was still a prominent feature in oocytes clamped precisely at the chloride equilibrium potential (data not shown); these results argue strongly that this component is not simply due to activation of Ca^{2+}-gated Cl^- channels.[2] In barium Ringer solution the second peak was reduced, but in larger responses an additional, slowly developing, inward current became apparent. This current could be abolished by BAPTA injections (see also Ref. 40). The reason for the reduction in the second component could be block or slow permeation by Ba^{2+} through NMDA receptor channels, whereas the additional, slow, Ca^{2+}-dependent current probably arises through Ba^{2+}-stimulated release of intracellular Ca^{2+} and resultant indirect activation of Cl^- channels. Unless stated otherwise, electrical recordings in the present study were made in normal frog Ringer solution, the initial spike of Cl^- current was ignored, and response amplitudes for pharmacological assays were measured at the peak of the slow phase (Fig. 2, *upper*). We considered this a reasonable approximation to current flowing directly through NMDA receptors under steady state desensitizing conditions.

Preliminary dose-response experiments established that 100 μM NMDA and 10 μM glycine provided saturation of the glutamate and glycine recognition sites (Figs. 2 and 3). At these concentrations, current levels ranged from 54 to 820 nA (mean ± standard error, 258 ± 58 nA; n = 16). Antagonist

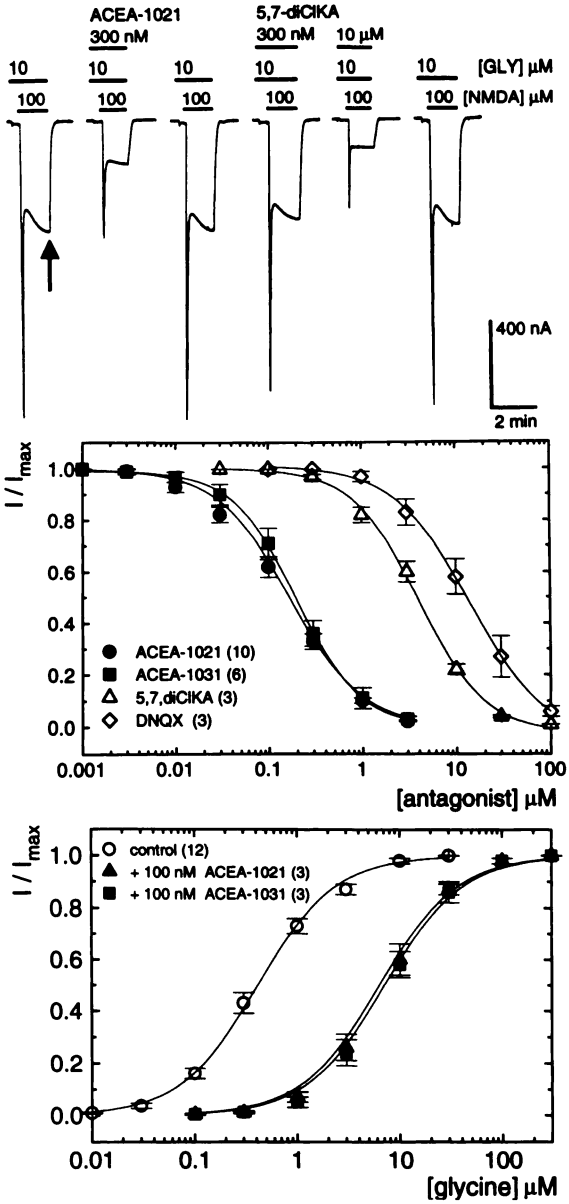

Fig. 2. *Upper*, sample records from a single oocyte, comparing potencies of ACEA-1021 and 5,7-diClKA against NMDA responses at receptors expressed by rat whole-brain poly(A)$^+$ RNA. Unless stated otherwise, the holding potential in this and the following figures is −70 mV. *Downward deflections*, inward current; *bars*, solution changes and drug applications. The dead time of the perfusion system was 5–10 sec. Responses were separated by 5–10-min intervals of wash (not shown). For pharmacological assays the initial spike of Cl^- current was ignored, and response amplitudes were measured at the peak of the slow phase (*arrow*). *GLY*, glycine. *Middle*, concentration-inhibition curves comparing potencies of ACEA-1021, ACEA-1031, 5,7-diClKA, and DNQX at NMDA receptors expressed by rat whole-brain poly(A)$^+$ RNA. NMDA was used at 100 μM and glycine at 10 μM. In this and all following figures data are plotted as the mean ± standard error, expressed as a fraction of either control responses (concentration-inhibition curves) or maximum responses (concentration-response curves). The number of separate experiments (cells) is given in parentheses. *Smooth curves*, best fits of eq. 3 to the data for each drug; see Materials and Methods for details. Curve parameters (IC_{50} and slope values) for these fits are given in Table 1. *Lower*, effects of 100 nM ACEA-1021 and ACEA-1031 on glycine concentration-response curves for NMDA receptors expressed by rat whole-brain poly(A)$^+$ RNA. The NMDA concentration was 100 μM. *Smooth curves*, best fits of eq. 2 to the data for each drug. Curve parameters (EC_{50} values for control curves and optimal slope values for paired curves for control and with drug) are given in Table 1.

[2] R. M. Woodward, unpublished observations.

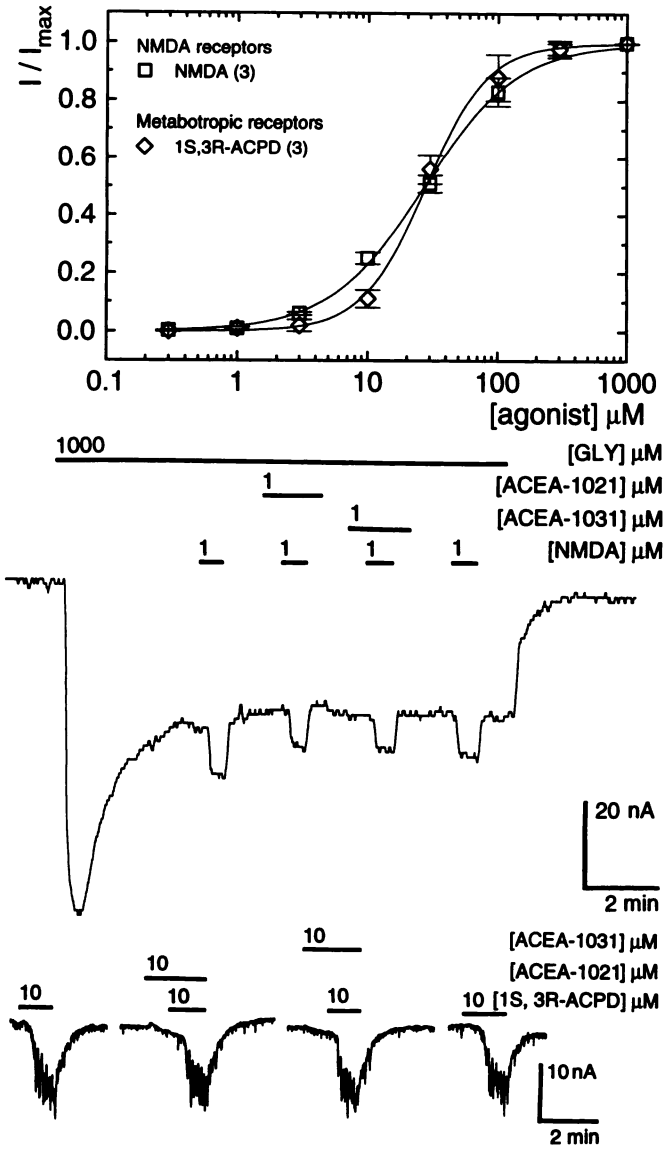

Fig. 3. *Upper*, concentration-response curves for NMDA at NMDA receptors and for (1*S*,3*R*)-ACPD at metabotropic glutamate receptors, in oocytes expressing rat whole-brain poly(A)$^+$ RNA. *Smooth curves*, best fits of eq. 1 to the data for each agonist. EC_{50} values and slope values are given in Table 1. *Middle* and *lower*, sample records from experiments designed to test whether ACEA-1021 or ACEA-1031 showed measurable inhibitory effects either at NMDA receptor glutamate binding sites or at metabotropic receptor glutamate binding sites. *Middle*, application of 1 mM glycine (*GLY*) elicited a membrane current response predominantly due to activation of strychnine-sensitive glycine receptors that are coexpressed by the rat brain poly(A)$^+$ RNA. This response was allowed to desensitize to steady state levels and used as a base-line for measuring currents mediated by NMDA receptors. Repeated coapplications of 1 μM NMDA elicited threshold NMDA responses (*downward notches in the record*) that were used to assay inhibition by antagonists. *Lower*, an oocyte was repeatedly exposed to 10 μM (1*S*,3*R*)-ACPD, eliciting a reproducible, threshold, oscillatory, Cl^- current, upon which ACEA-1021 and ACEA-1031 were assayed for inhibition.

potency was initially assessed using fixed agonist concentrations (100 μM NMDA and 10 μM glycine) and varying concentrations of inhibitor. In all cases, oocytes were pretreated with glycine for approximately 30 sec and receptors were then activated by coapplication of NMDA. Antagonists were applied together with glycine to promote equilibration before receptor activation. Even when high concentrations of antagonists were used, inhibition was washed out fully within ~5 min. To verify the ongoing level of control responses, which showed variability, oocytes were regularly tested with NMDA and glycine in the absence of antagonist.

As shown in Fig. 2, *middle*, concentration-inhibition curves for ACEA-1021 and ACEA-1031 indicated potent antagonism at rat brain NMDA receptors expressed in oocytes. For both compounds the IC_{50} was between 150 and 200 nM. This value represents roughly 20-fold higher potency than that of 5,7-diClKA and nearly 100-fold higher potency than that of DNQX assayed in the same cells (Table 1, *upper*). Slopes of inhibition curves were in the range of −1.3 to −1.1, giving no indication of a pharmacologically heterogeneous population of receptors.

The mechanism of inhibition was investigated by measuring the effects of fixed concentrations of ACEA-1021 and ACEA-1031 (100 nM) on the concentration-response relation for glycine. Both compounds caused parallel rightward shifts in the glycine concentration-response relation, with approximately 20-fold increases in the EC_{50} and no clear reductions in the maximum response (Fig. 2). Effects of both drugs were consistent with competitive inhibition at the glycine binding site (ACEA-1021, $F_{1,116} = 2.6$; ACEA-1031, $F_{1,44} = 3.3$). Assuming simple competitive antagonism for all four antagonists (28, 30, 32), the EC_{50} for glycine measured under control conditions was used in conjunction with IC_{50} values to estimate K_b values using a Leff-Dougall approach (38). For comparison, shifts in EC_{50} induced by fixed concentrations of ACEA-1021 and ACEA-1031 were used to calculate K_b values, using the Gaddum-Schild relationship (24). There was good agreement between the two methods of analysis (Table 1).

Preliminary experiments in oocytes suggested that inhibition by ACEA-1021 and ACEA-1031 showed little or no voltage dependence over the range of −20 to −100 mV. However, extending the voltage range to positive potentials was complicated by activation of large endogenous currents. A more thorough study of the voltage dependence of inhibition was performed using neuronal NMDA responses (see below).

The ability of 100 μM glycine to completely overcome inhibition produced by 100 nM ACEA-1021 (Fig. 2) was consistent with preliminary binding studies that suggested that ACEA-1021 was relatively inactive at glutamate recognition sites on NMDA receptors.[3] Electrophysiological assays were therefore designed simply to test whether any inhibitory actions could be detected at the glutamate binding site. The protocol used a high concentration of glycine (1 mM), to promote saturation at glycine sites, whereas NMDA was used at concentrations (1–3 μM) sufficient to elicit threshold responses, thereby maximizing the chances of detecting inhibition at glutamate sites. Under these conditions, ACEA-1021 and ACEA-1031 at concentrations of up to 1 μM showed <25% inhibition of NMDA responses (e.g., Fig. 3). Using the EC_{50} for NMDA of ~27 μM (Fig. 3; Table 1, *lower*) and assuming a competitive interaction, we estimated the K_b for both antagonists at glutamate binding sites to be >2 μM, i.e., 150–200-fold lower than affinities at glycine sites. These experiments were complicated, a little, by activation of classical strychnine-sensitive glycine receptors that are coexpressed in oocytes injected with rat brain poly(A)$^+$ RNA. The glycine re-

[3] E. Weber, unpublished observations.

TABLE 1

Inhibition by ACEA-1021, ACEA-1031, 5,7-diClKA, and DNQX of rat brain glutamate receptors expressed in oocytes

Upper, analysis of concentration-inhibition experiments. Current amplitudes were normalized with respect to control responses and pooled. IC_{50} and slope values are from the best fits of the data to eq. 3. K_b values were estimated using a Leff-Dougall approach, a generalized form of the Cheng-Prusoff relationship (see Materials and Methods). Fixed agonist concentrations are indicated. For NMDA receptor glycine site assays, the NMDA concentration was 100 μM. *Lower*, analysis of concentration-response experiments. Current amplitudes were normalized with respect to maximum currents and pooled. EC_{50} values for control curves (in the absence of antagonist) and slope values are from the best fits of the data to eq. 2. K_b values were estimated, using the Gaddum-Schild relationship, from parallel rightward shifts in agonist concentration-response curves induced by fixed concentrations of antagonist (see Materials and Methods). Data are given as the mean, quoted to two significant figures. Numbers in parentheses are 95% confidence intervals. *n* indicates the number of separate experiments (i.e., the number of cells examined). Unless otherwise stated, this presentation applies to Tables 2 and 3.

Receptor	Agonist	Antagonist	IC_{50}	Concentration-inhibition curve slope	K_b (Leff-Dougall)	*n*
			μM		μM	
NMDA	Glycine (10 μM)	ACEA-1021	0.17 (0.15, 0.20)	−1.1 (−1.3, −0.95)	0.0068 (0.006, 0.008)	10
		ACEA-1031	0.2 (0.17, 0.23)	−1.3 (−1.3, −1.2)	0.008 (0.007, 0.01)	6
		5,7-DiClKA	3.8 (3.5, 4.2)	−1.3 (−1.3, −1.2)	0.16 (0.14, 0.17)	3
		DNQX	12 (10, 16)	−1.1 (−1.4, −0.85)	0.51 (0.4, 0.64)	3
Non-NMDA	AMPA (10 μM)	ACEA-1021	1.7 (1.7, 1.8)	−1.1 (−1.2, −1.0)	1.8 (1.7, 1.9)	3
		ACEA-1031	1.3 (1.2, 1.4)	−1.1 (−1.2, −1.0)	1.3 (1.2, 1.4)	3
		5,7-DiClKA	32 (26, 40)	−1.1 (−1.2, −1.0)	34 (28, 42)	3
		DNQX	0.32 (0.31, 0.34)	−1.3 (−1.4, −1.2)	0.34 (0.32, 0.36)	4
Non-NMDA	Kainate (20 μM)	ACEA-1021	0.76 (0.71, 0.81)	−1.3 (−1.4, −1.2)	1.5 (1.4, 1.6)	4
		ACEA-1031	0.54 (0.50, 0.57)	−1.2 (−1.3, −1.1)	1 (0.9, 1.1)	3
		5,7-DiClKA	17 (16, 18)	−1.3 (−1.4, −1.2)	32 (30, 34)	3
		DNQX	0.12 (0.11, 0.12)	−1.2 (−1.3, −1.1)	0.24 (0.22, 0.26)	3

Receptor	Agonist	Antagonist	EC_{50} (control curve)	Concentration-response curve slope	K_b (Gaddum-Schild)	*n*
			μM		μM	
NMDA	Glycine	ACEA-1021	0.41 (0.38, 0.45)	1.2 (1.1, 1.3)	0.0063 (0.005, 0.008)	3
		ACEA-1031	0.54 (0.46, 0.63)	1.2 (1.1, 1.3)	0.0075 (0.006, 0.01)	3
NMDA	NMDA		27 (23, 31)	1.2 (0.77, 1.7)		3
Non-NMDA	AMPA	ACEA-1021	8.8 (8.1, 9.7)	1.7 (1.5, 1.9)	1.1 (0.9, 1.4)	3
Non-NMDA	Kainate	ACEA-1021	85 (80, 91)	1.6 (1.5, 1.7)	1.3 (1.1, 1.5)	4
Metabotropic	ACPD		28 (24, 32)	1.8 (1.4, 2.3)		4

ceptor responses were either reduced using 10–30 μM strychnine or allowed to desensitize to a stable plateau level before applications of NMDA (Fig. 3).

NMDA receptors expressed by RNA transcribed from cloned rat cDNAs. Currents mediated by cloned rat NMDA receptors were similar to those observed with expression of whole-brain poly(A)$^+$ RNA. As described for the corresponding mouse subunits (13), cRNA combinations encoding NR1 and NR2 subunits resulted in strong expression of NMDA responses in oocytes. NR1A expressed alone produced relatively small currents, typically <5% of the current observed with combinations of subunits. NR2 subunits expressed alone failed to respond. Four different subunit combinations were studied in detail. In each case the NR1A subunit was combined with a single NR2 subunit, either NR2A, -2B, -2C, or -2D. The currents produced by these four combinations showed some differences in their time courses. All four subunit combinations gave rise to the initial transient Cl^- current described above, but the secondary peak of current tended to be more pronounced with the NR1A/2A and NR1A/2B combinations, compared with NR1A/2C or NR1A/2D. In addition, like the receptors expressed by rat brain poly(A)$^+$ RNA, NR1A/2A and NR1A/2B responses showed progressive run-down upon repeated application of agonists, often followed by a gradual increase in current during extended periods of recording. These slow changes in the levels of control responses were less pronounced in oocytes expressing NR1A/2C or -2D. Current ranges and mean maximum responses in concentration-response experiments were as follows: NR1A/2A, 64–217 nA (100 ± 19 nA, n = 8); NR1A/2B, 124–545 nA (304 ± 46 nA, n = 8); NR1A/2C, 66–765 nA (275 ± 229 nA, n = 7); NR1A/2D, 44–140 nA (91 ± 20 nA, n = 6). Levels of receptor expression were similar in other types of assays.

Following procedures described for oocytes expressing rat brain poly(A)$^+$ RNA, antagonism of NMDA receptors assembled from cloned subunits was first evaluated from concentration-inhibition curves using fixed levels of glycine and glutamate (10 μM and 100 μM, respectively). In terms of IC_{50} values, the four binary subunit combinations showed considerable variation in sensitivity to ACEA-1021 and ACEA-1031 (Fig. 4). The pattern was very similar for the two drugs; NR1A/2A receptors showed highest sensitivity (IC_{50} values of ~0.03 μM), NR1A/2B and -2C intermediate values (IC_{50} values of 0.1–0.5 μM), and NR1A/2D lowest sensitivity (IC_{50} values of >1 μM) (Table 2, *upper*). Slopes of inhibition curves ranged between −1.5 and −0.94. NR1A/2A gave slightly higher values (shallower slopes), compared with other combinations. With hindsight, we suspect that this was simply due to inaccurate assessment of control levels, as opposed to evidence for a heterogeneous population of receptors.

To investigate the mechanisms responsible for the variations in IC_{50} values, we measured the apparent affinity of the four subunit combinations for glycine. As previously reported for rat and mouse clones (12–14), glycine concentration-response curves for the different subunit combinations showed differences in apparent affinity (Fig. 4). NR1A/2A combinations showed the lowest sensitivity to glycine (EC_{50} values of ~1 μM), NR1A/2B and NR1A/2C intermediate values (EC_{50} values of ~0.2 μM), and NR1A/2D the highest affinity (EC_{50}

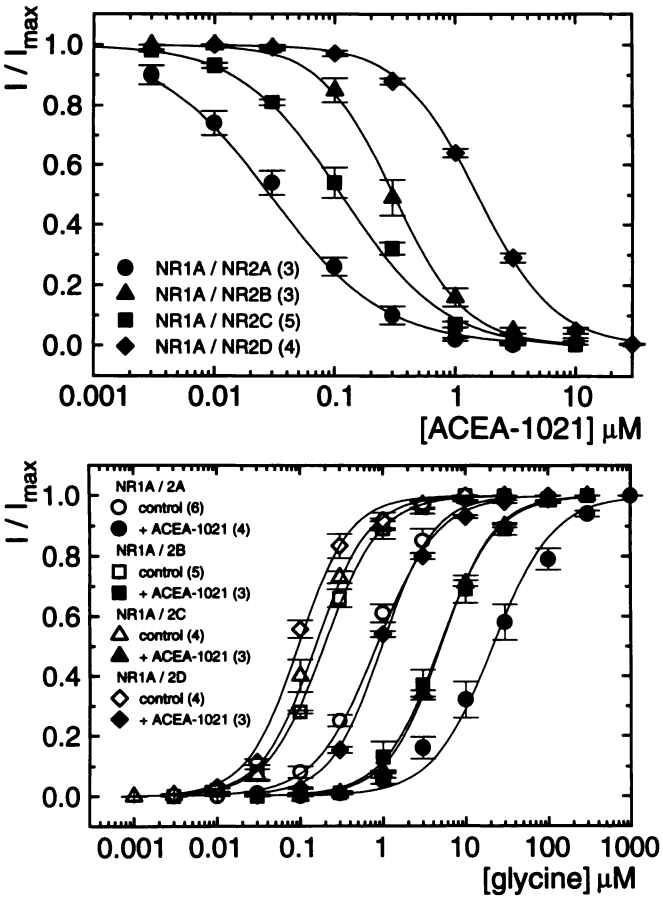

Fig. 4. *Upper*, concentration-inhibition curves showing the relative sensitivities of four cloned rat NMDA receptor subunit combinations to ACEA-1021 (glycine was used at 10 μM and glutamate at 100 μM). *Smooth curves*, best fits of eq. 3 to the data for each subunit combination. Curve parameters (IC_{50} and slope values) for these fits are given in Table 2. *Lower*, effect of 100 nM ACEA-1021 on concentration-response curves for glycine at four cloned rat NMDA receptor subunit combinations. The glutamate concentration was 100 μM. *Smooth curves*, best fits of eq. 2 to the data for each subunit combination. With the exception of NR1A/2C (see Fig. 5), EC_{50} values for control curves and optimal slope values for paired curves are given in Table 2.

values of ~0.1 μM) (Table 2, *lower*). Occasionally (~1 in 10 frogs) there were batches of oocytes that expressed NR1A/2A receptors with atypically high sensitivity to glycine (EC_{50} values of 0.1–0.2 μM). The factors responsible for this difference in receptor properties remain unclear. Subsequent injections of cRNA into oocytes from the same frogs resulted in receptors with similar atypical properties, suggesting that some oocytes either show abnormal post-translational processing/regulation of receptors or express endogenous receptor components that are electrically silent in uninjected cells. In the present study, data from atypical oocytes were excluded from analysis.

Glycine concentration-response curves for the four subunit combinations all showed parallel shifts with fixed concentrations of ACEA-1021 and ACEA-1031 (Fig. 4). K_b values were estimated from inhibition curves and from displacement of glycine concentration-response relations (Table 2); the two methods showed close agreement. NR1A/2C appears to have the highest affinity for ACEA-1021 and ACEA-1031 (K_b values of 2–3 nM), NR1A/2A and NR1A/2B slightly lower values (K_b values of 3–4 nM and 4–9 nM, respectively), and NR1A/2D the lowest antagonist affinities (K_b values of 11–13 nM).

The strong antagonism of NR1A/2A receptors expressed in terms of IC_{50} values is, therefore, due to their low affinity for glycine and relatively high affinity for ACEA-1021 and ACEA-1031. On the other hand, IC_{50} values for NR1A/2D receptors indicate weak antagonism because this subunit combination has the highest affinity for glycine and the lowest affinity for the antagonists. In these experiments all antagonism was consistent with the simple competitive model except for inhibition of NR1A/2A by ACEA-1021 ($F_{1,69} = 9.8$), which resulted in a slightly lower slope for the glycine concentration-response relation in the presence of the antagonist (Fig. 4). Oocytes injected with NR1A/2A displayed the greatest variability in their control responses, and we strongly suspect that the slight reduction in slope observed with ACEA-1021 was due to this variability, rather than to some additional complexity in inhibitory mechanism. It should be noted that inhibition of NR1A/2A by ACEA-1031 was consistent with the simple competitive model ($F_{1,79} = 2.1$).

As a more stringent test of inhibitory mechanism, we performed a Schild analysis for ACEA-1021 at NR1A/2C using four antagonist concentrations (Fig. 5). ACEA-1021 showed no significant deviation from the simple competitive model over the concentration range of 10–300 nM ($F_{7,113} = 1.2$). A Schild regression plot of EC_{50} dose ratios versus ACEA-1021 concentration had a slope of 1.0 ± 0.02 ($n = 3$).

Following the protocol described for whole-brain NMDA receptors, actions of ACEA-1021 and ACEA-1031 at glutamate sites were assessed using concentrations of glutamate sufficient to elicit threshold responses (0.03–0.3 μM, depending on subunit combination) and a high saturating concentration of glycine (1 mM). At concentrations of up to 1 μM, neither antagonist caused >30% inhibition of the responses (data not shown). In terms of a competitive interaction, these experiments indicate that K_b values for ACEA-1021 and ACEA-1031 at glutamate binding sites on all four subunit combinations are >2 μM.

Membrane currents recorded in oocytes expressing NR1A alone were uniformly small (slow phase, <20 nA) (11) and showed run-down, so it was difficult to make detailed pharmacological measurements. Nonetheless, the EC_{50} for glycine at the putative NR1A homo-oligomeric receptor was typically between 0.1 and 0.3 μM. ACEA-1021 and ACEA-1031 inhibited responses elicited by 100 μM glutamate and 1 μM glycine with IC_{50} values ranging between 30 and 100 nM. Inhibition appeared to be fully surmounted by increasing glycine concentrations. Assuming a simple competitive mechanism, these results imply K_b values at homo-oligomeric NR1A receptor glycine sites in the range of ~5–10 nM, i.e., similar to the values obtained for the hetero-oligomeric receptors. When hetero-oligomeric NR1A/NR2 receptors are expressed, small subpopulations of homo-oligomeric NR1A receptors, if present, would not overtly distort calculation of K_b values. Possible actions of ACEA-1021 and ACEA-1031 at glutamate sites on homo-oligomeric receptors were not investigated.

Non-NMDA receptors expressed by rat whole-brain poly(A)$^+$ RNA. Two agonists, AMPA and kainate, were used to activate non-NMDA glutamate receptors expressed by rat whole-brain poly(A)$^+$ RNA. As described previously (28), the time courses of membrane currents evoked by these two

TABLE 2

Inhibition by ACEA-1021 of cloned rat NMDA receptors expressed in oocytes

Upper, analysis of concentration-inhibition experiments. IC_{50} and slope values are from the best fits of the data to eq. 3. K_b values were estimated using a Leff-Dougall approach (see Materials and Methods). *Lower*, analysis of concentration-response experiments. EC_{50} values for control curves and slope values are from the best fits of the data to eq. 2. K_b values were estimated using the Gaddum-Schild relationship (see Materials and Methods). Glutamate was used 100 μM in all experiments.

Receptor subunits	IC_{50}, ACEA-1021	Concentration-inhibition curve slope	K_b (Leff-Dougall)	*n*
	nM		nM	
NR1A/2A	29 (15, 56)	−0.94 (−1.1, −0.82)	2.8 (2.4, 3.2)	3
NR1A/2B	300 (260, 350)	−1.4 (−1.7, −1.2)	5.9 (5.1, 6.7)	3
NR1A/2C	120 (100, 140)	−1.1 (−1.2, −0.9)	1.9 (1.6, 2.2)	5
NR1A/2D	1500 (1400, 1600)	−1.4 (−1.5, −1.3)	11 (10, 12)	4
Receptor subunits	EC_{50}, glycine (control curve)	Concentration-response curve slope	K_b (Gaddum-Schild)	*n*
	nM		nM	
NR1A/2A	840 (730, 960)	1.1 (1, 1.2)	4 (3.2, 5)	4
NR1A/2B	193 (170, 220)	1.3 (1.2, 1.4)	4.2 (3.5, 5)	3
NR1A/2C	150 (140, 160)	1.3 (1.3, 1.4)	2.8 (2.6, 3.1)	3[a]
NR1A/2D	96 (87, 110)	1.4 (1.3, 1.5)	11 (9.3, 13)	3

[a] Data for inhibition of NR1A/2C by ACEA-1021 are from simultaneous fitting of the more extensive Schild-type experiments shown in Fig. 5, *upper*.

agonists in oocytes were relatively simple. Maximum steady state responses to AMPA were typically <10% of the maximum currents elicited by kainate in the same oocyte. Coapplication of AMPA to cells with pre-established kainate responses resulted in occlusion of the kainate currents, indicating that, to a large extent, the two agonists interact with a common pool of non-NMDA glutamate receptors.[4] This result is consistent with numerous neuronal studies that have demonstrated strong desensitization of non-NMDA receptors by AMPA but relatively little desensitization by kainate (e.g., Ref. 41). Application of drugs to the oocytes by conventional bath perfusion is too slow to elicit the initial peak of current seen in neurons with fast perfusion techniques; instead, AMPA responses measured in oocytes represent current flow through non-NMDA receptors under steady state desensitizing conditions. Kainate activates substantially the same population of non-NMDA receptors as does AMPA but produces less desensitization and thus a larger steady state current. In general, kainate and AMPA responses were more reproducible than NMDA currents, so control applications of agonist alone were required less often. Current ranges and mean maximum responses measured in the concentration-response experiments for AMPA and kainate were 100–280 nA (176 ± 36 nA, $n = 5$) and 292-2350 nA (1516 ± 930 nA, $n = 5$), respectively.

ACEA-1021 and ACEA-1031 were initially tested against fixed concentrations of AMPA (10 μM, ~50% I_{max}) and kainate (20 μM, ~10% I_{max}). Oocytes were pretreated with antagonist for approximately 30 sec before application of agonist (Fig. 6, *upper*). Inhibition of non-NMDA responses by ACEA-1021 or ACEA-1031 was fully washed out within a few minutes of drug application. Concentration-inhibition curves showed that the relative potencies of ACEA-1021, ACEA-1031, DNQX, and 5,7-diClKA at non-NMDA receptors clearly differed from the pattern at NMDA receptors (Fig. 6). Using either AMPA or kainate as the agonist, DNQX was the strongest inhibitor at non-NMDA receptors (IC_{50} values of approximately 0.3 and 0.1 μM, respectively), being 4–6 times more active than ACEA-1021 and ACEA-1031 and 100–150 times more active than 5,7-diClKA (Table 1, *upper*).

[4] R. M. Woodward, unpublished observations.

The mechanism of inhibition was investigated by measuring effects of a fixed concentration of ACEA-1021 on agonist concentration-response relationships. EC_{50} values for AMPA and kainate (Table 1, *lower*) were increased roughly 3–4-fold in the presence of the drug. At 3 μM, ACEA-1021 caused parallel rightward shifts in the concentration-response curves for AMPA that were consistent with competitive inhibition ($F_{1,45} = 0.68$) (Fig. 6). Antagonism of oocyte kainate responses, although largely surmountable, appeared to show a small component of noncompetitive inhibition. This component was <5% of the total response but was sufficient to cause significant departure from the competitive model ($F_{1,50} = 11.8$). We suspect that this deviation is simply due to inadequate monitoring of maximum response levels. Although the inhibitory action of ACEA-1031 was not tested across full concentration-response curves for kainate and AMPA, antagonism by the drug (at 3 μM) was substantially surmountable (data not shown). K_b values were calculated from concentration-inhibition curves and from the rightward displacement of agonist dose-response relations (Table 1). There was good correlation between values obtained by the two methods.

One complicating factor in these experiments was that currents evoked by AMPA reached a maximum at ~100 μM, whereas higher concentrations (pH adjusted) produced currents that were 5–20% smaller in amplitude (42). (The same phenomenon probably occurred with kainate responses but was less pronounced.) For reasons that are unclear, declines in response at high AMPA concentrations were not wholly offset by ACEA-1021. As a result, maximal currents recorded with 3 μM ACEA-1021 were never as large as maximal control responses. Instead, currents in the presence of 3 μM ACEA-1021 approached saturation at reduced amplitudes corresponding to the control responses produced by supramaximal concentrations of AMPA. For purposes of curve fitting, currents evoked by AMPA alone were plotted as a fraction of the response to 100 μM AMPA; the response to 300 μM AMPA, although actually smaller, was also considered maximal. Currents measured in the presence of 3 μM ACEA-1021 were plotted as a fraction of the response to 300 μM AMPA (Fig. 6).

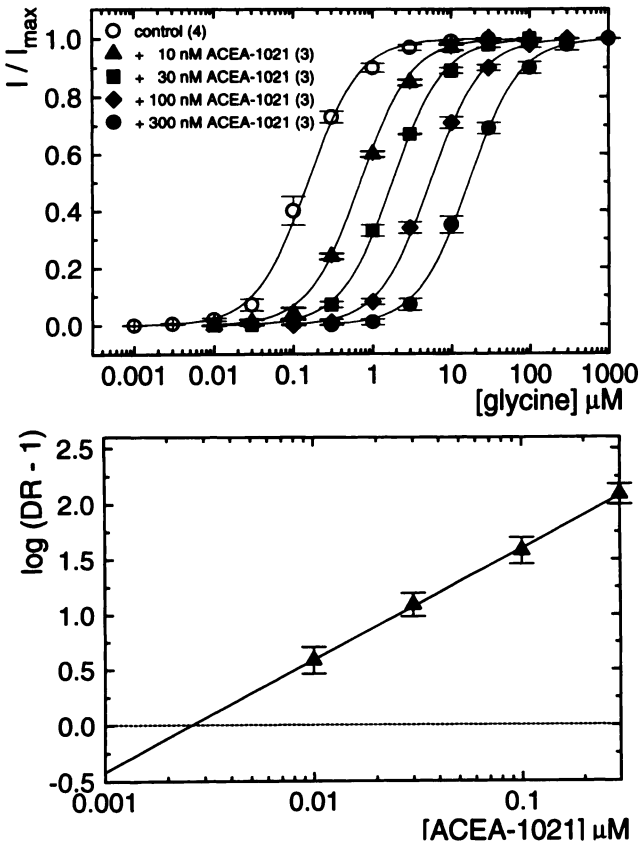

Fig. 5. *Upper*, effects of four concentrations of ACEA-1021 on concentration-response curves for glycine in oocytes expressing the NR1A/NR2C subunit combination. Glutamate was used at 100 μM. *Smooth curves*, best fits of eq. 2 to the data. The EC_{50} value for the control curve and the optimal slope values for all five curves are given in Table 2. *Lower*, Schild regression of the same data. Dose ratios were calculated from EC_{50} values for each curve fitted independently with eq. 1. *DR*, dose ratio. The *line* was fitted by linear regression (slope = 1.0, K_b = 2.8 nM) (see Table 2).

Metabotropic glutamate receptors expressed by rat whole-brain poly(A)$^+$ RNA. Metabotropic glutamate receptors comprise a family of G protein-coupled receptors (43). The receptors expressed in oocytes were selectively activated using the agonist (1*S*,3*R*)-ACPD (44). The resulting currents were inward at a holding potential of −70 mV and were characterized by long latencies (particularly when low concentrations of agonist were used) and a fluctuating/oscillatory time course (Fig. 3). Numerous previous studies have shown that responses of this type arise from receptor-mediated stimulation of the phosphoinositide/Ca^{2+} pathway, which activates endogenous Cl^- channels to produce the oscillating current detected under voltage-clamp conditions (37, 44). At −70 mV, maximum (1*S*,3*R*)-ACPD responses for concentration-response experiments ranged between 180 and 490 nA (330 ± 90 nA, n = 3).

Quantitative pharmacological characterization of metabotropic receptors was made difficult by receptor desensitization and by run-down of the response over time. In addition, activation of the Cl^- current exhibited a strong threshold effect, so curve parameters showed dependence on the level of receptor expression as well as other factors. Nonetheless, to provide a rough gauge of agonist affinity at the metabotropic receptors, concentration-response curves were measured for

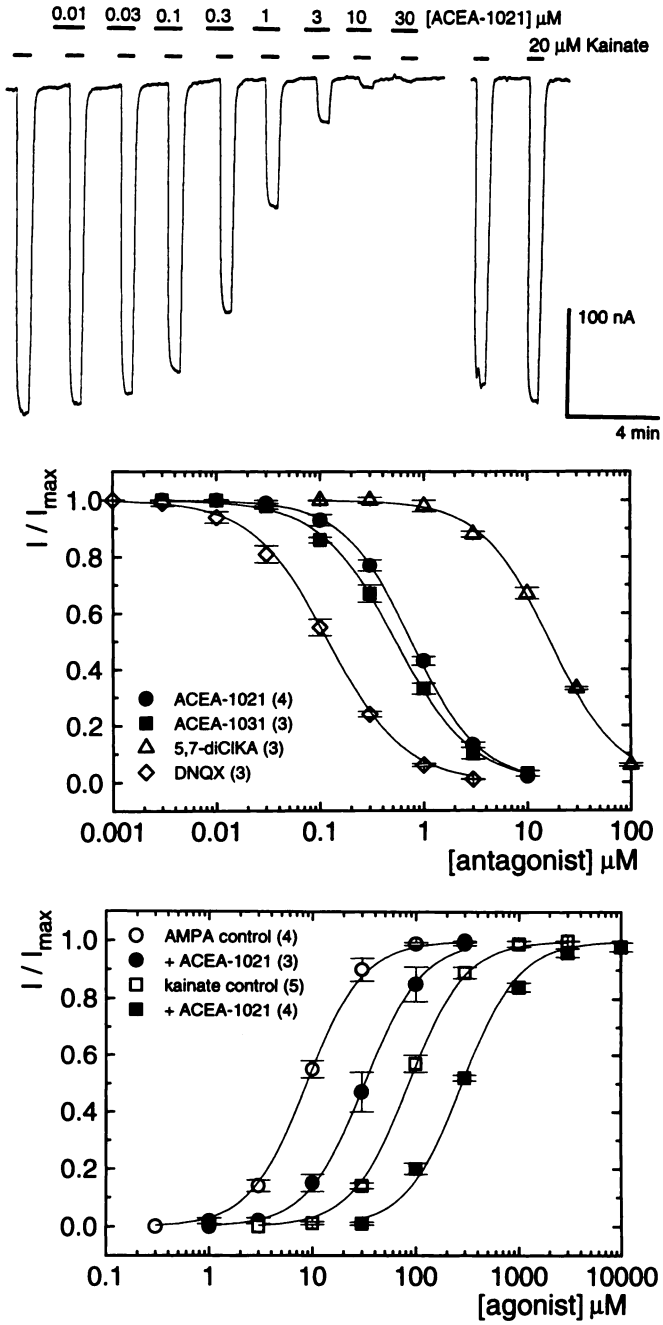

Fig. 6. *Upper*, sample records illustrating inhibition of kainate responses by ACEA-1021 in an oocyte expressing rat whole-brain poly(A)$^+$ RNA. After exposure to 30 μM ACEA-1021, the oocyte required 2–3 min of additional washing before the response fully returned to control. *Middle*, concentration-inhibition curves comparing potencies of ACEA-1021, ACEA-1031, 5,7-diClKA, and DNQX at non-NMDA receptors activated by kainate. *Smooth curves*, best fits of eq. 3 to the data for each drug. IC_{50} and slope values for these fits are given in Table 1. *Lower*, effect of ACEA-1021 (3 μM) on concentration-response curves for AMPA and kainic acid. *Smooth curves*, best fits of eq. 2 to the data for each agonist. EC_{50} values for control curves and optimal slope values for paired curves are given in Table 1.

(1*S*,3*R*)-ACPD (Fig. 3; Table 1, *lower*). ACEA-1021 and ACEA-1031 were tested against low (5–10 μM) concentrations of (1*S*,3*R*)-ACPD because these doses produced more reproducible responses and maximized the potential for detecting competitive inhibition. Neither drug caused apprecia-

ble antagonism under these conditions, even when applied at concentrations as high as 10 or 30 μM (Fig. 3, *lower*). In terms of competitive inhibition, this result implies that K_b values for ACEA-1021 and ACEA-1031 at metabotropic glutamate receptors are >50 μM.

Electrical Recordings from Cultured Rat Cortical Neurons

NMDA receptor assays. Whole-cell currents evoked by 100 μM NMDA plus various concentrations of glycine were recorded from rat cortical neurons in culture, at a holding potential of −70 mV and in the absence of external Mg^{2+}. During each agonist application, the current initially rose to a peak and then declined over a period of several seconds (Fig. 7, *upper*, *inset*). Amplitude measurements were made during the final phase of the response, when the current approached a steady state level. With saturating glycine concentrations the steady state currents ranged from 327 to 2470 pA (1097 ± 179 pA, n = 15).

For direct comparison with results from the oocyte recordings, antagonist potency was initially evaluated by coapplication of fixed doses of NMDA (100 μM) and glycine (1 μM) with increasing concentrations of antagonist. ACEA-1021 produced complete inhibition of whole-cell NMDA currents at 1 μM. The IC_{50} was ~40 nM (Table 3). Although not investigated in detail, ACEA-1031 appeared to have a similar IC_{50} at neuronal NMDA receptors. Concentration-response relations for glycine applied with 100 μM NMDA, or with NMDA plus 100 nM ACEA-1021, provided evidence for potent antagonism at the glycine binding site (Fig. 7). The control EC_{50} of ~180 nM is in line with previous work on central nervous system neurons in culture (7, 24). Inhibition by ACEA-1021 was completely surmountable by increasing glycine concentrations and produced a 20-fold increase in the EC_{50} for glycine, which was consistent with the competitive model ($F_{1,44}$ = 1.1). As described above, K_b values for ACEA-1021 at the glycine site were calculated from antagonist inhibition curves and from the parallel shift in the concentration-response relation for glycine (Table 3).

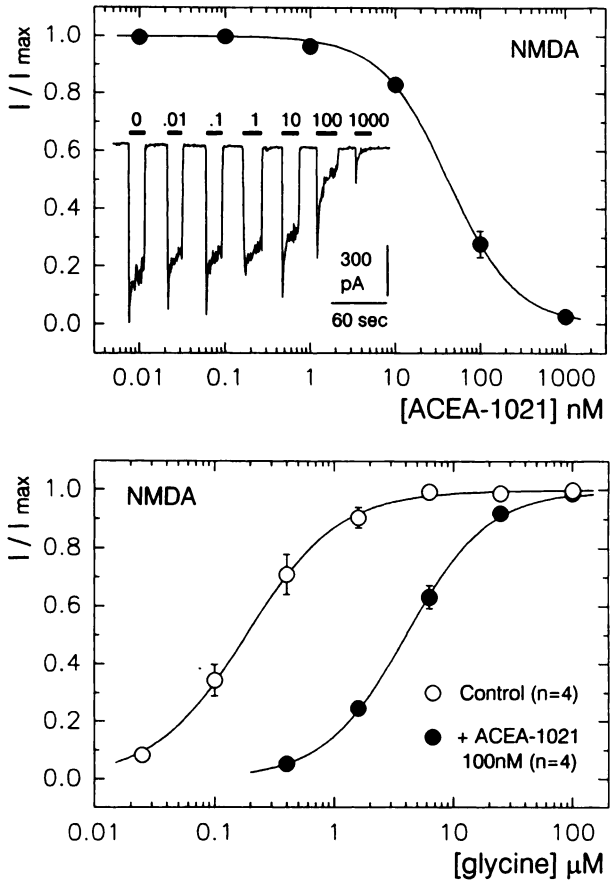

Fig. 7. Inhibition of whole-cell currents gated by NMDA plus glycine in cultured rat cortical neurons. *Upper*, concentration-inhibition curve for ACEA-1021. NMDA was used at 100 μM and glycine at 1 μM (n = 4). *Smooth curve*, best fit of eq. 3 to the data. IC_{50} and slope values are given in Table 3. *Inset*, sample records illustrating the inhibitory action of ACEA-1021, which was applied together with NMDA and glycine as indicated (*solid bars*). *Numbers above the bars*, antagonist concentrations (in μM). *Lower*, effect of 100 nM ACEA-1021 on the concentration-response relation for glycine. The NMDA concentration was 100 μM (n = 4). *Smooth curves*, best fits of eq. 2 to the data. EC_{50} values for control curves and optimal slope values for the pair of curves are given in Table 3.

The voltage dependence of ACEA-1021 and ACEA-1031 effects at NMDA receptors was assessed by comparing levels of inhibition of responses at two holding potentials, −60 mV and +40 mV. When assayed against responses elicited by 100 mM NMDA and 1 mM glycine, 100 nM ACEA-1021 caused 82.6 ± 2.3% inhibition at −60 mV and 81.4 ± 3% inhibition at +40 mV (n = 3). Assayed under the same conditions, ACEA-1031 caused 84.8 ± 1.5% inhibition at −60 mV and 81 ± 2.3% inhibition at +40 mV (n = 3). Neither drug showed any appreciable dependence on voltage.

Non-NMDA receptor assays. Kainate and AMPA were applied to cultured neurons clamped at a holding potential of −70 mV. Both agonists evoked inward currents at this potential, ranging from 138 to 1788 pA for kainate (736 ± 115 pA, n = 15) and from 71 to 1700 pA for steady state currents activated by AMPA (834 ± 165 pA, n = 15). As described previously (41), currents activated by relatively high doses of AMPA (>50 μM) displayed an initial peak that rapidly desensitized to a stable plateau, whereas currents evoked by kainate were maintained throughout the application, without any evidence of desensitization (Fig. 8, *upper* and *middle*, *insets*). In all cases, inhibition produced by ACEA-1021 was evaluated for steady state currents during the final third of each agonist application.

As with NMDA and glycine, ACEA-1021 was first tested against responses elicited by fixed concentrations of AMPA and kainate. Half-maximal inhibition of whole-cell current gated by 5 μM AMPA required ~4 μM ACEA-1021, whereas the IC_{50} against 100 μM kainate was ~2 μM (Table 3). At a fixed concentration of 5 μM, ACEA-1021 produced parallel rightward shifts in the concentration-response curves for both AMPA and kainate (Fig. 8). In each case, the EC_{50} was increased by roughly 3-fold, whereas the maximal responses to AMPA (250 μM) and kainate (10 mM) were unchanged by the drug. Apparent dissociation constants for ACEA-1021 at neuronal non-NMDA receptors were calculated assuming competitive inhibition, for AMPA responses, $F_{1,41}$ = 0.85; for kainate responses, $F_{1,56}$ = 0.068 (Table 3). These experiments indicated that ACEA-1021 is considerably less potent at neuronal non-NMDA receptors than at NMDA receptor glycine sites. The voltage dependence of inhibition at non-NMDA receptors was not investigated.

TABLE 3

Inhibition by ACEA-102 of NMDA and non-NMDA receptors in cultured rat cortical neurons

Upper, analysis of concentration-inhibition experiments. IC_{50} and slope values are from the best fits of the data to eq. 3. K_b values were estimated using a Leff-Dougall approach (see Materials and Methods). Fixed agonist concentrations are indicated. For NMDA receptor glycine site assays the NMDA concentration was 100 μM. *Lower*, analysis of concentration-response experiments. EC_{50} values for control curves and slope values are from the best fits of the data to eq. 2. K_b values were estimated using the Gaddum-Schild relationship (see Materials and Methods).

Receptor	Agonist	IC_{50}, ACEA-1021	Concentration-inhibition curve slope	K_b (Leff-Dougall)	*n*
		μM		μM	
NMDA	Glycine (1 μM)	0.042 (0.035, 0.05)	−1.1 (−1.3, −0.9)	0.0071 (0.006, 0.0084)	4
Non-NMDA	AMPA (5 μM)	3.9 (3.3, 4.6)	−1.1 (−1.3, −1.0)	3.3 (2.8, 4.0)	5
Non-NMDA	Kainate (100 μM)	1.7 (1.6, 1.9)	−1.2 (−1.2, −1.0)	1.5 (1.3, 1.6)	4
Receptor	Agonist	EC_{50} (control curve)	Concentration-response curve slope	K_b (Gaddum-Schild)	*n*
		μM		μM	
NMDA	Glycine	0.18 (0.16, 0.21)	1.2 (1.1, 1.3)	0.0048 (0.0039, 0.006)	4
Non-NMDA	AMPA	4.2 (3.8, 4.7)	1.5 (1.3, 1.6)	2.2 (1.7, 2.7)	5
Non-NMDA	Kainate	150 (130, 170)	1.6 (1.0, 1.3)	2.3 (1.8, 3)	6

Discussion

Pharmacology of quinoxalinediones. Quinoxalinediones were initially characterized as selective antagonists for AMPA-preferring non-NMDA receptors (35, 27). Subsequent work has shown that these molecules can also be moderately potent inhibitors at glycine allosteric sites on NMDA receptors (3, 26, 28, 33). The present experiments indicate that potency of quinoxalinediones at NMDA glycine sites and selectivity with respect to non-NMDA receptors are both critically dependent on the type and pattern of benzene ring substitutions. In particular, the 5-nitro-6,7-dichloro (ACEA-1021) and 5-nitro-6,7-dibromo (ACEA-1031) derivatives of 1,4-dihydro-2,3-quinoxalinedione are shown to be highly potent and selective glycine site antagonists.

Inhibition at NMDA receptors. Results obtained in oocyte assays for NMDA receptors expressed by rat whole-brain poly(A)$^+$ RNA (Table 1) or cloned receptor subunits (Table 2) were in reassuringly close agreement with the data from cultured rat cortical neurons (Table 3). Electrophysiological assays in oocytes and neurons showed that inhibition of NMDA receptors by ACEA-1021 is consistent with a simple competitive interaction at the glycine coagonist site. Recordings from oocytes indicated that ACEA-1031 inhibits responses at the NMDA receptor by the same mechanism. Like other glycine site antagonists (24), there was no indication of voltage dependence in the inhibition produced by either drug. In all assays the apparent affinities of ACEA-1021 and ACEA-1031 for glycine sites were in the low nanomolar range. K_b values estimated from concentration-inhibition curves consistently showed close correlation with values obtained from the more conventional Schild-type experiments. So, at least for these types of assays, the Leff-Dougall approach appears to be a quick and reliable means of estimating antagonist potencies. Although RNA preparations were not identical (e.g., whole brain versus cerebral cortex), apparent affinities of the control compounds 5,7-diClKA and DNQX were comparable to values calculated in previous studies (28, 45).

Agreement between oocyte assays using rat whole-brain poly(A)$^+$ RNA and assays using cloned NMDA receptor subunits indicates that any additional uncharacterized subunits or splice variants present in the poly(A)$^+$ RNA either have sensitivity to ACEA-1021 and ACEA-1031 similar to that of the clones or are present in sufficiently small amounts to have little influence on the net potency of the drugs. Agreement between data from clones expressed in oocytes and data from neurons suggests that, with respect to glycine site pharmacology, the simple hetero-oligomeric NR1A/NR2 subunit combinations correspond closely to neuronal NMDA receptors.

Oocyte recordings failed to detect inhibition by ACEA-1021 and ACEA-1031 at glutamate binding sites. These types of experiments were limited by the potency of actions at glycine sites, and selectivity could only be estimated as at least 100–200-fold. Preliminary binding studies, on the other hand, indicated that affinities at NMDA receptor glutamate binding sites are no lower than ~30 μM,[5] i.e., that both compounds display >1000-fold selectivity for the glycine site, relative to the glutamate site. This is consistent with previous studies showing that other quinoxalinediones are weakly active as conventional competitive NMDA receptor antagonists (3, 25).

Selectivity at different NMDA receptor subtypes. In terms of actual affinities, ACEA-1021 and ACEA-1031 showed only modest (up to 5-fold) levels of true subunit selectivity at the four putative NMDA receptor subtypes expressed in oocytes (Table 2). Indeed, compared with a drug such as ifenprodil (40), ACEA-1021 and ACEA-1031 should be considered broad-spectrum antagonists across NMDA receptor subtypes. However, for these antagonists IC_{50} values may give a more relevant measure of *in vivo* actions. From this perspective, using fixed agonist concentrations, ACEA-1021 and ACEA-1031 showed up to 50-fold variations in activity. This was due to the conjunction of subunit-dependent differences in apparent glycine affinity and differences in affinity for the antagonists themselves.

If NMDA receptor subtypes corresponding to these subunit combinations exist in mammalian brain, then our results suggest that ACEA-1021, ACEA-1031, and related glycine site antagonists would show distinct patterns of subtype-selective activity. For example, at a uniform glycine concentration, receptors composed of NR1A/2A subunits would be 5–10 times more sensitive to ACEA-1021 than receptors composed of NR1A/2B or NR1A/2C and ~50 times more sensitive than receptors composed of NR1A/2D. If glycine levels show

[5] E. Weber, unpublished observations.

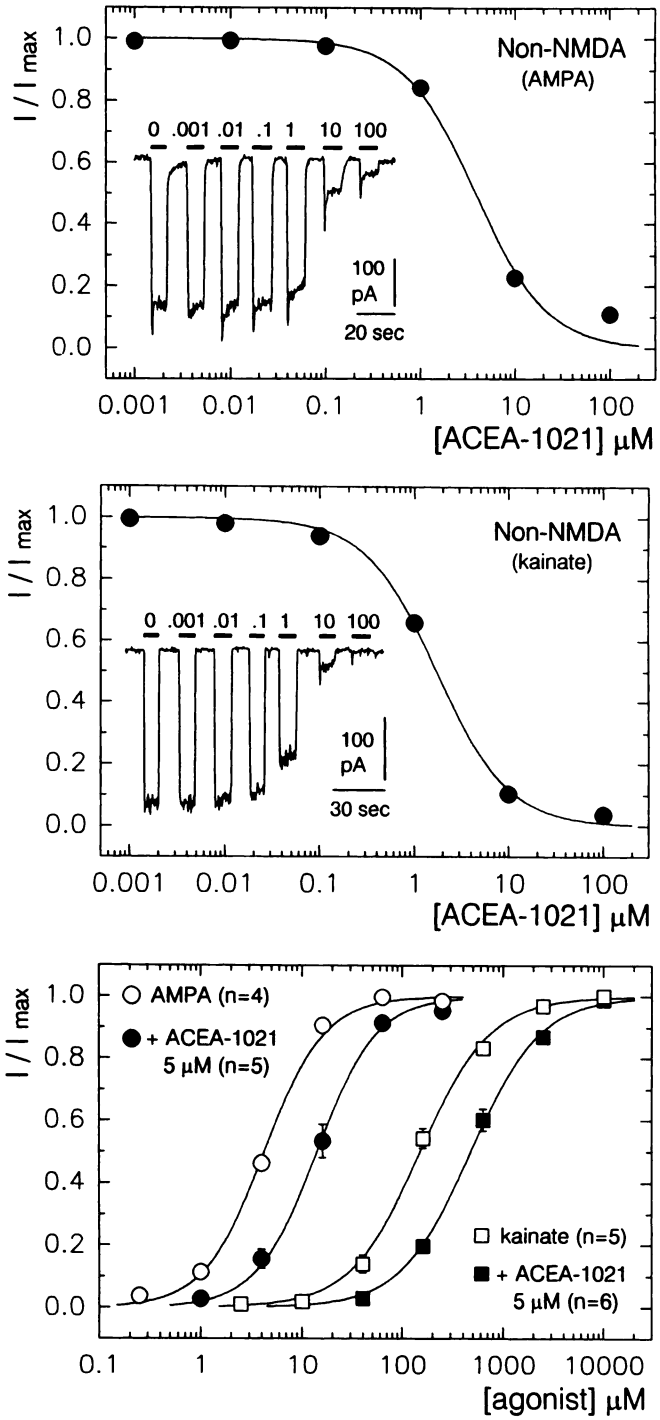

Fig. 8. Inhibition of currents activated by kainate and AMPA in cultured rat cortical neurons. *Upper*, concentration-inhibition curve for ACEA-1021 with a fixed concentration of 5 μM AMPA (n = 5). *Smooth curve*, best fit of eq. 3 to the data. IC_{50} and slope values are given in Table 3. *Inset*, sample records showing inhibition of AMPA currents by increasing concentrations of ACEA-1021. *Black bars*, periods of simultaneous agonist and antagonist application. *Numbers above the bars*, concentrations of ACEA-1021 (in μM). *Middle*, concentration-inhibition curve for ACEA-1021 with 100 μM kainate (n = 4). *Smooth curve*, best fit of eq. 3 to the data. IC_{50} and slope values are given in Table 3. *Inset*, sample experiment illustrating inhibition of kainate-induced current by ACEA-1021. *Lower*, effects of 5 μM ACEA-1021 on the steady state concentration-response relations for AMPA (n = 5) and kainate (n = 6). *Smooth curves*, best fits of eq. 2 to the data for both agonists. EC_{50} values for control curves and optimal slope values for pairs of curves are given in Table 3.

local variability, this could either accentuate or diminish the functional selectivity of the antagonists. Modest differential subtype sensitivities of this type may be sufficient to influence the therapeutic and behavioral profiles of glycine site antagonists (e.g., Refs. 21, 22, and 35).

Inhibition at non-NMDA receptors. Both ACEA-1021 and ACEA-1031 showed clear inhibition of non-NMDA receptors. There was close agreement between oocyte and neuronal data with respect to inhibitory mechanism and potency. In both assay systems, antagonism of AMPA responses by ACEA-1021 was consistent with simple competitive inhibition at the glutamate binding site. Inhibition of kainate responses showed some deviation from the competitive model in oocyte assays but was consistent in neuronal assays. The major component of current evoked by kainate, in both oocytes and neurons, was inhibited with roughly the same potency as the current elicited by AMPA. In all assays, ACEA-1021 blocked responses to AMPA or kainate with K_b values that ranged between ~1 and 3 μM.

The potency of DNQX at non-NMDA receptors expressed in oocytes was similar to that measured previously (28). Oocyte assays also confirmed that, although kynurenic acids are relatively weak inhibitors at non-NMDA receptors, this class of molecules is not wholly inactive (3, 32, 45).

Effects at metabotropic glutamate receptors. Oocyte electrophysiological assays suggest that, in contrast to ionotropic receptors, metabotropic receptors are effectively insensitive to ACEA-1021 and ACEA-1031. Apparent affinities at the metabotropic receptors expressed by rat brain poly(A)$^+$ RNA were no lower than 50 μM, representing >5000-fold lower potencies than those at NMDA receptor glycine sites. It should be noted, however, that the oocyte experiments were able to assay only metabotropic receptors that were positively coupled to the phosphoinositide/Ca^{2+} pathway (37, 43, 44). Studies at the molecular level have now identified six subtypes of metabotropic receptors, together with various splice variants (43). Characterization of the different subtypes suggests that primarily metabotropic receptor types 1 and 5 would be involved in activating oocyte electrical responses (43, 44). Although it seems unlikely, there remains the possibility that ACEA-1021 or ACEA-1031 interacts with subtypes of metabotropic receptors that do not participate in the oocyte responses.

Structure-activity considerations. As described in the introduction, a burgeoning number of compounds have been identified as NMDA receptor glycine site antagonists (18, 19, 23, 24, 28–31). Since the pioneering studies on kynurenic acids, it has been recognized that substitutions on the benzene ring, common to all of the antagonists, have a strong influence on affinity (18, 19, 23). Our own results emphasize that for quinoxaline-2,3-diones the type and pattern of benzene ring substitutions are critical in determining the potency of glycine site antagonism and also the selectivity of antagonism versus non-NMDA receptors.

Comparison of K_b values for ACEA-1021 and ACEA-1031 with the respective values obtained for related mono- and disubstituted quinoxalinediones reveals a striking synergism between the nitro group at position 5 and the halogens at positions 6 and 7 (for the most direct comparisons, the K_b values given below are our own unpublished data from oocytes expressing rat whole-brain poly(A)$^+$ RNA, but see also Refs. 3, 23, and 28 for previously reported affinities). Using

the nitro/chloro series for illustration, the unsubstituted parent compound, 1,4-dihydro-2,3-quinoxalinedione, has low potency at NMDA and non-NMDA receptors (K_b values of ~17 and 100 μM, respectively). Nitro substitution at position 5 has little or no effect on potency at glycine sites and causes some reduction in activity at non-NMDA receptors. Separately substituting chloro at positions 6 and 7 of the parent molecule results in a 40-fold increase in potency at glycine sites (K_b ~ 0.4 μM) and a 25-fold increase at non-NMDA receptors (K_b ~ 5 μM). Combining these substitutions to generate ACEA-1021 yields a 60-fold increase in potency against glycine, compared with 6,7-dichloro-1,4-dihydroquinoxaline-2,3-dione, as well as an additional ~20-fold increase in selectivity for glycine sites versus non-NMDA receptors. Reasons why these ternary substitution patterns are so favorable for glycine site binding are not clear. Although the parameters involved are almost certainly complex, one factor influencing potency could be the orientation of the 5-nitro group. In ACEA-1021 and ACEA-1031 the 5-nitro group is directed out of the plane of the ring, due to orthosteric hindrance. Increased potency may be due to additional hydrogen bonding becoming available at this position.

Selectivity of antagonism *in vivo*. We consider it unlikely that ACEA-1021 and ACEA-1031 have any appreciable *in vivo* actions at NMDA receptor glutamate binding sites or at metabotropic glutamate receptors. The situation with respect to non-NMDA glutamate receptors is, however, more complex. In common with other quinoxalinediones (3, 25, 27, 28), our experiments indicate that ACEA-1021 and ACEA-1031 inhibit non-NMDA receptors, in this instance with low micromolar affinities. Simply with respect to potency, these drugs can therefore be considered as dual-activity ionotropic glutamate receptor antagonists. On the other hand, the high potency of inhibition at glycine binding sites appears to provide a strong selectivity index in favor of antagonism at NMDA receptors, yielding 100–500-fold greater potency at glycine sites than at non-NMDA receptors (Tables 1 and 3). Although these values suggest selective antagonism at NMDA receptors, they may not provide an accurate picture of the "functional activity" of ACEA-1021 and ACEA-1031 *in vivo*, by which we mean the ability of the drugs to block excitatory postsynaptic currents, as opposed to their affinity for a particular binding site.

Most models of excitatory synaptic physiology assume (perhaps incorrectly) that glycine in synaptic clefts is fixed at low micromolar or submicromolar concentrations. Antagonists such as ACEA-1021 and ACEA-1031 would be expected to compete under steady state conditions against this prevailing concentration of glycine. In contrast, except for a low background level, glutamate is present in the cleft only during synaptic activation. Thus, with respect to non-NMDA receptor inhibition, ACEA-1021 and ACEA-1031 would reach equilibrium with the residual background levels of glutamate present at rest. Upon synaptic activation glutamate levels are transiently raised into the millimolar range, but these high concentrations of agonist persist for only a few milliseconds (46). The ability of glutamate to displace ACEA-1021 and ACEA-1031 thus would depend on the kinetics of antagonist unbinding. Slow rates of drug dissociation would tend to increase the functional activity at non-NMDA receptors and thus erode the selectivity index measured under steady state conditions. For example, if we assume that the high glutamate concentrations achieved upon synaptic release are too transient to displace ACEA-1021 from non-NMDA receptors, then the "functional selectivity index" at a concentration of 1 μM glycine would be reduced from ~200-fold to 50-fold. Hippocampal slice recordings assaying related quinoxalinediones provide evidence that these types of effects are indeed relevant (28). Characterization of the synaptic pharmacology of ACEA-1021 and ACEA-1031 will be needed to assess the extent to which such considerations influence antagonist selectivity *in vivo*. In addition, the present experiments did not investigate ACEA-1021 or ACEA-1031 for any potential subtype selectivity at non-NMDA receptors (8), which could further complicate their pharmacological profiles.

Possible therapeutic implications. At present, the principal therapeutic indication for NMDA receptor antagonists is as neuroprotectants in the treatment of ischemic stroke and head trauma (15). Evidence indicates that NMDA receptors play a pivotal role in excitotoxicity, a pathological phenomenon wherein extended exposure to glutamate causes overactivation of neurons and subsequent cell death (47). Excitotoxicity appears to be responsible for substantial amounts of the brain damage incurred after stroke-induced ischemia or head trauma and it is now generally accepted that NMDA receptor antagonists are neuroprotective in models of focal ischemia (26, 48). In addition, non-NMDA receptor antagonists also seem to have neuroprotective properties. For example, 2,3-dihydroxy-6-nitro-7- sulfamoylbenzo(F)quinoxaline, a potent and highly selective non-NMDA receptor antagonist, has neuroprotective actions in rat global ischemia (49), a model in which NMDA receptor antagonists appear to be ineffective (50).

Concurrent studies indicate that ACEA-1021 and ACEA-1031 have robust neuroprotective actions in a rat model of focal ischemia (34). The present results indicate that these compounds inhibit both NMDA and non-NMDA receptors. Steady state selectivity indices suggest that the major sites of action *in vivo* are NMDA receptors, and this is consistent with their apparent lack of activity in a rat global ischemia model (34). Still, it remains possible that inhibition at non-NMDA receptors does contribute to neuroprotective efficacy; even modest inhibition at non-NMDA receptors could synergistically suppress activity at excitatory synapses and hence augment levels of protection.

References

1. Johnston, J. W., and P. Ascher. Glycine potentiates the NMDA response of mouse central neurones. *Nature (Lond.)* **325**:529–531 (1987).
2. Kleckner, N. W., and R. Dingledine. Requirement for glycine in activation of *N*-methyl-D-aspartic acid receptors expressed in *Xenopus* oocytes. *Science (Washington D. C.)* **241**:835–837 (1988).
3. Yoneda, Y., and K. Ogita. Abolition of an NMDA-mediated response by a specific glycine antagonist, 6,7-dichloroquinoxaline-2,3-dione (DCQX). *Biochem. Biophys. Res. Commun.* **164**:841–849 (1989).
4. Mayer, M. L., L. Vyklicky, and J. Clements. Regulation of NMDA receptor desensitization in mouse hippocampal neurons by glycine. *Nature (Lond.)* **338**:425–427 (1989).
5. Monaghan, D. T., H. J. Olverman, L. Nguyen, J. C. Watkins, and C. W. Cotman. Two classes of *N*-methyl-D-aspartate recognition sites: differential distribution and differential regulation by glycine. *Proc. Natl. Acad. Sci. USA* **85**:9836–9840 (1988).
6. Lester, R. A. J., G. Tong, and C. E. Jahr. Interactions between glycine and glutamate binding sites on the NMDA receptor. *J. Neurosci.* **13**:1088–1096 (1993).
7. Vyklicky, L., M. Benveniste, and M. L. Mayer. Modulation of *N*-methyl-D-aspartic acid receptor desensitization by glycine in mouse cultured hippocampal neurones. *J. Physiol. (Lond.)* **428**:313–331 (1990).
8. Hollmann, M., and S. Heinemann. Cloned glutamate receptors. *Annu. Rev. Neurosci.* **17**:31–108 (1994).

9. Ben-Ari, Y., E. Cherubini, and K. Krnjevic. Changes in voltage-dependence of NMDA currents during development. *Neurosci. Lett.* **94**:88–92 (1988).
10. Moriyoshi, K., M. Masu, T. Ishii, R. Shigemoto, N. Mizuno, and S. Nakanishi. Molecular cloning and characterization of the rat NMDA receptor. *Nature (Lond.)* **354**:31–37 (1991).
11. Sugihara, H., K. Moriyoshi, T. Ishii, M. Masu, and S. Nakanishi. Structures and properties of seven isoforms of NMDA receptor generated by alternative splicing. *Biochem. Biophys. Res. Commun.* **185**:826–832 (1992).
12. Monyer, H., R. Sprengel, R. Schoepfer, A. Herb, M. Higuchi, H. Lomeli, N. Burnashev, B. Sakmann, and P. H. Seeburg. Heteromeric NMDA receptors: molecular and functional distinction of subtypes. *Science (Washington D. C.)* **256**:1217–1221 (1992).
13. Kutsuwada, T., N. Kashiwabuchi, H. Mori, K. Sakimua, E. Kushiya, K. Araki, H. Meguro, H. Masaki, T. Kumanihsi, M. Arakawa, and M. Mishina. Molecular diversity of the NMDA receptor channel. *Nature (Lond.)* **358**:36–41 (1992).
14. Monyer, H., N. Burnashev, D. J. Laurie, B. Sakmann, and P. H. Seeburg. Developmental and regional expression in the rat brain and functional properties of four NMDA receptors. *Neuron* **12**:529–540 (1994).
15. McCulloch, J. Excitatory amino acid antagonists and their potential for the treatment of ischeamic brain damage in man. *Br. J. Clin. Pharamcol.* **34**:106–114 (1992).
16. Rogawski, M. A. The NMDA receptor, NMDA antagonists and epilepsy therapy. *Drugs* **44**:279–292 (1992).
17. Wilcox, G. L. Excitatory neurotransmitters and pain, in *Proceedings of the VIth World Congress on Pain* (M. R. Bond, J. E. Charlton, and C. J. Woolf, eds.). Elsevier Science Publishers, Amsterdam, 97–117 (1991).
18. Huettner, J. E. Competitive antagonism of glycine at the *N*-methyl-D-aspartate (NMDA) receptor. *Biochem. Pharmacol.* **41**:9–16 (1991).
19. Kemp, J. A., and P. D. Leeson. The glycine site of the NMDA receptor: five years on. *Trends Pharmacol. Sci.* **14**:20–25 (1993).
20. Hargreaves, R. J., M. Rigby, D. Smith, and R. G. Hill. Lack of effect of L-687–414 ((+)-*cis*-4-methyl-HA-966), an NMDA receptor antagonist acting at the glycine site, on cerebral glucose metabolism and cortical neuronal morphology. *Br. J. Pharmacol.* **110**:36–42 (1993).
21. Singh, L., R. Menzies, and M. D. Tricklebank. The discriminative stimulus properties of (+)-HA-966, an antagonist at the glycine/*N*-methyl-D-aspartate receptor. *Eur. J. Pharmacol.* **186**:129–132 (1990).
22. Koek, W., and F. C. Colpaert. *N*-Methyl-D-aspartate antagonism and phencyclidine-like activity: behavioral effects of glycine site ligands, in *Multiple Sigma and PCP Receptor Ligands: Mechanisms for Neuromodulation and Neuroprotection* (J.-M. Kamenka and E. F. Domino, eds.). CPP Books, Ann Arbor, MI, 665–671 (1992).
23. Leeson, P. D. Glycine-site *N*-methyl-D-aspartate receptor antagonists, in *Drug Design for Neuroscience* (A. P. Kozikowski, ed.). Raven Press, New York, 339–381 (1993).
24. Swartz, K. J., W. J. Koroshetz, A. H. Rees, and J. E. Huettner. Competitive antagonism of glutamate receptor channels by substituted benzazepines in cultured cortical neurons. *Mol. Pharmacol.* **41**:1130–1141 (1992).
25. Honore, T. G., S. N. Davies, J. Drejer, E. J. Fletcher, P. Jacobsen, D. Lodge, and F. E. Nielsen. Quinoxalinediones: potent competitive non-NMDA glutamate receptor antagonists. *Science (Washington D. C.)* **241**:701–703 (1988).
26. Birch, P. J., C. J. Grossman, and A. G. Hayes. 6,7-Dinitro-quinoxaline-2,3-dione and 6-nitro-7-cyano-quinoxaline-2,3-dione antagonize responses to NMDA in the rat spinal cord by an action at the strychnine-insensitive glycine receptor. *Eur. J. Pharmacol.* **156**:177–180 (1988).
27. Fletcher, E. J., D. Martin, J. A. Aram, D. Lodge, and T. Honore. Quinoxalinediones selectively block quisqualate and kainate receptors and synaptic events in rat neocortex and hippocampus and frog spinal cord *in vitro*. *Br. J. Pharmacol.* **95**:585–597 (1988).
28. Randle, J. C. R., T. Guet, C. Bobichon, C. Moreau, P. Curutchet, B. Lambolez, L. Prado De Carvalho, A. Cordi, and J. M. Lepagnol. Quinoxaline derivatives: structure-activity relationships and physiological implications of inhibition of *N*-methyl-D-aspartate and non-*N*-methyl-D-aspartate receptor-mediated currents and synaptic potentials. *Mol. Pharmacol.* **41**:337–345 (1992).
29. Rowley, M., P. D. Leeson, G. I. Stevenson, A. M. Moseley, I. Stansfield, I. Sanderson, L. Robinson, R. Baker, J. A. Kemp, G. R. Marshall, A. C. Foster, S. Grimwood, M. D. Tricklebank, and K. L. Saywell. 3-Acyl-4-hydroxyquinolin-2(1*H*)-ones: systemically active anticonvulsants acting by antagonism at the glycine site of the *N*-methyl-D-aspartate receptor complex. *J. Med. Chem.* **36**:3386–3396 (1993).
30. Carling, R. W., P. D. Leeson, K. W. Moore, J. D. Smith, C. R. Moyes, I. M. Mawer, S. Thomas, T. Chan, R. Baker, A. C. Foster, S. Grimwood, J. A. Kemp, G. R. Marshall, M. D. Tricklebank, and K. L. Saywell. 3-Nitro-3,4-dihydro-2(1*H*)-quinilones: excitatory amino acid antagonists acting at the glycine site NMDA and (*RS*)-α-amino-3-hydroxy-5-methyl-4-isoxazolepropionic acid receptors. *J. Med. Chem.* **36**:3397–3408 (1993).
31. Kulagowski, J. J., R. Baker, N. R. Curtis, P. D. Leeson, I. M. Mawer, A. M. Moseley, M. P. Ridgill, M. Rowley, I. Stansfield, A. C. Foster, S. Grimwood, R. G. Hill, J. A. Kemp, G. R. Marshall, K. L. Saywell, and M. D. Tricklebank. 3′-(Arylmethyl)- and 3′-(aryloxy)-3-phenyl-4-hydroxyquinolin-2(1*H*)-ones: orally active antagonists of the glycine site on the NMDA receptor. *J. Med. Chem.* **37**:1402–1405 (1994).
32. Kleckner, N. W., and R. Dingledine. Selectivity of quinoxalines and kynurenines as antagonists of the glycine site on *N*-methyl-D-aspartate receptors. *Mol. Pharmacol.* **36**:430–436 (1989).
33. Lester, R. A. J., M. L. Quarum, J. D. Parker, E. Weber, and C. E. Jahr. Interaction of 6-cyano-7-nitroquinoxaline-2,3-dione with the *N*-methyl-D-aspartate receptor-associated glycine binding site. *Mol. Pharmacol.* **35**:565–570 (1989).
34. Warner, D. S., H. Martin, P. Ludwig, A. McAllister, J. F. W. Keana, and E. Weber. *In vivo* models of cerebral ischemia: effects of parenterally administered NMDA receptor glycine site antagonists. *J. Cereb. Blood Flow Metab.* **15**:188–196 (1995).
35. Balster, R. L., D. M. Grech, R. S. Mansbach, H. Li, and E. Weber. Behavioral studies on the novel glycine-site NMDA antagonists ACEA-1011 and ACEA-1021 in rats. *Soc. Neurosci. Abstr.* **19**:472 (1993).
36. Woodward, R. M., L. Polenzani, and R. Miledi. Effects of steroids on γ-aminobutyric acid receptors expressed in *Xenopus* oocytes by poly(A)$^+$ RNA from mammalian brain and retina. *Mol. Pharmacol.* **41**:89–103 (1992).
37. Miledi, R., and I. Parker. Chloride current induced by injection of calcium in *Xenopus* oocytes. *J. Physiol. (Lond.)* **357**:173–183 (1984).
38. Leff, P., and I. G. Dougall. Further concerns over Cheng-Prusoff analysis. *Trends Pharmacol. Sci.* **14**:110–112 (1993).
39. Leonard, J. P., and S. R. Kelso. Apparent desensitization of NMDA responses in *Xenopus* oocytes involves calcium-dependent chloride current. *Neuron* **2**:53–60 (1990).
40. Williams, K. Ifenprodil discriminates subtypes of the *N*-methyl-D-aspartate receptor: selectivity and mechanisms at recombinant heteromeric receptors. *Mol. Pharmacol.* **44**:851–859 (1993).
41. Kiskin, N. I., O. A. Krishtal, and A. Y. Tsydrenko. Excitatory amino acid receptors in hippocampal neurons: kainate fails to desensitize them. *Neurosci. Lett.* **63**:255–266 (1990).
42. Geoffroy, M., B. Lambolez, E. Audinat, B. Hamon, F. Crepel, J. Rossier, and R. Kado. Reduction of desensitization of a glutamate ionotropic receptor by antagonists. *Mol. Pharmacol.* **39**:587–591 (1991).
43. Schoepp, D. D., and P. J. Conn. Metabotropic glutamate receptors in brain function and pathology. *Trends Pharmacol. Sci.* **14**:13–20 (1993).
44. Manzoni, O., L. Fagni, J.-P. Pin, F. Rassendren, F. Poulat, F. Sladeczek, and J. Bockaert. (*trans*)-1-Aminocyclopentyl-1,3-dicarboxylate stimulates quisqualate phosphoinositide-coupled receptors but not ionotropic glutamate receptors in striatal neurons and *Xenopus* oocytes. *Mol. Pharmacol.* **38**:1–6 (1990).
45. McNamara, D., E. C. R. Smith, D. O. Calligaro, P. J. O'Malley, L. A. McQuaid, and R. Dingledine. 5,7-Dichlorokynurenic acid, a potent and selective competitive antagonist of the glycine site on NMDA receptors. *Neurosci. Lett.* **120**:17–20 (1990).
46. Clements, J. D., R. A. Lester, G. Tong, C. E. Jahr, and G. L. Westbrook. The time course of glutamate in the synaptic cleft. *Science (Washington D. C.)* **258**:1498–1501 (1992).
47. Choi, D. W., and S. M. Rothman. The role of glutamate neurotoxicity in hypoxic-ischemic neuronal death. *Annu. Rev. Neurosci.* **13**:171–182 (1990).
48. Parke, C. K., D. G. Nehls, D. I. Graham, G. M. Teasdale, and J. McCulloch. Focal ischemia in the cat: treatment with the glutamate antagonist MK-801 after induction of ischemia. *J. Cereb. Blood Flow Metab.* **8**:757–762 (1988).
49. Sheardown, M. J., E. O. Neilsen, A. J. Hansen, P. Jacobsen, and T. Honore. 2,3-Dihydro-6-nitro-7-sulfamoyl-benzo(*f*)quinoxaline: a neuroprotectant for cerebral ischemia. *Science (Washington D. C.)* **247**:571–574 (1990).
50. Sheardown, M. J., P. D. Suzdak, and L. Nordholm. AMPA, but not NMDA, antagonism is neuroprotective in gerbil global ischemia, even when delayed 24h. *Eur. J. Pharmacol.* **236**:347–352 (1993).

Send reprint requests to: R. M. Woodward, Acea Pharmaceuticals, 1003 Health Sciences Road West, Irvine, CA 92715.